Developmental and Comparative Immunology 161 (2024) 105252

Contents lists available at ScienceDirect

Developmental and Comparative Immunology

journal homepage: www.elsevier.com/locate/devcompimm

SRP54 of black carp negatively regulates MDA5-mediated antiviral innate immunity

Jixiang Chu, Yixia Chen, Yanfang Wu, Wei Qin, Jun Yan **, Jun Xiao *, Hao Feng

State Key Laboratory of Developmental Biology of Freshwater Fish, College of Life Science, Hunan Normal University, Changsha, 410081, China

ARTICLE INFO

Keywords:
SRP54
MDA5
SVCV
Black carp
Innate immunity

ABSTRACT

Signal Recognition Particle 54 kDa (SRP54) is a subunit of the signal recognition particle (SRP), a cytoplasmic ribonucleoprotein complex guiding the transportation of newly synthesized proteins from polyribosomes to endoplasmic reticulum. In mammals, it has been reported to regulate the RLR signaling pathway negatively by impairing the association between MAVS and MDA5/RIG-I. However, the role of SRP54 in teleost antiviral innate immune response remains obscure. In this study, the SRP54 homolog of black carp (bcSRP54) has been cloned, and its function in antiviral innate immunity has been elucidated. The CDS of *bcSRP54* gene consists of 1515 nucleotides and encodes 504 amino acids. Immunofluorescence (IF) showed that bcSRP54 was mainly distributed in the cytoplasm. Overexpressed bcSRP54 significantly reduced bcMDA5-mediated transcription of interferon (IFN) promoter in reporter assay. Co-expression of bcSRP54 and bcMDA5 significantly suppressed bcMDA5-mediated IFN signaling and antiviral activity, while bcSRP54 knockdown increased the antiviral ability of host cells. In addition, the results of the immunofluorescence staining demonstrated the subcellular overlapping between bcSRP54 and bcMDA5, and the co-immunoprecipitation (co-IP) experiment identified their association. Furthermore, the over-expression of bcSRP54 did not influence the protein expression and ubiquitination modification level of bcMDA5, however, hindered the binding of bcMDA5 to bcMAVS. In summary, our results conclude that bcSRP54 targets bcMDA5 and inhibits the interaction between bcMDA5 and bcMAVS, thereby negatively regulating antiviral innate immunity, which provides insight into how teleost SRP54 regulates IFN signaling.

1. Introduction

The innate immune response plays a crucial role in protecting against viral infections. The recognition of the pathogen-associated molecular pattern (PAMP) of invading pathogenic microorganisms through pattern recognition receptors (PRRS) is a key step in activating the host's innate immune response (Kawai et al., 2024; Li, 2021). RIG-I like receptor (RLR) is the key PPRs for discerning RNA viruses and initiating the antiviral response, which is composed of three main members: RIG-I (Retinoic acid-inducible gene I), MDA5 (Melanoma differentiation-associated gene 5), and LGP2 (Laboratory of Genetics and Physiology 2) (Chunhaphinyokul et al., 2023; Rehwinkel, 2020). Studies in mammals have shown that RIG-I preferentially binds to short double-stranded RNA (dsRNA) (less than 1 kb) and 5-triphosphate dsRNA, whereas MDA5 preferentially recognizes long dsRNA (more than 2 kb) (Kato et al., 2008; Lian et al., 2018). Upon binding to dsRNA, both RIG-I and MDA5 can undergo a conformational change, leading to its activation and subsequent interaction with the adaptor protein MAVS (Mitochondrial antiviral signaling protein) (Fan and Jin, 2019; Sharma et al., 2021; Wei, 2020). This interaction triggers the activation of downstream signaling cascades, ultimately producing type I interferons (IFNs) and other inflammatory cytokines (Kowalinski et al., 2011). All RLRs possess a central helicase domain and a so-called carboxy-terminal domain (CTD) that work together to detect immunostimulatory RNA (Rehwinkel, 2020). RIG-I and MDA5 also contain two amino-terminal caspase activation and recruitment domains (CARDs), facilitating downstream signal transduction (Duic et al., 2020). However, LGP2 lacks the CARDs, it is typically responsible for regulating the RLR signaling pathway (Li et al., 2021; Sanchez David et al., 2019).

Fish also have three conserved RLR receptors and the RLRs recognize

* Corresponding author. State Key Laboratory of Developmental Biology of Freshwater Fish, College of Life Science, Hunan Normal University, Changsha, Hunan, 410081, China.
** Corresponding author.
E-mail addresses: yj1214@hunnu.edu.cn (J. Yan), xiaojun@hunnu.edu.cn (J. Xiao).

https://doi.org/10.1016/j.dci.2024.105252
Received 14 June 2024; Received in revised form 17 August 2024; Accepted 17 August 2024
Available online 21 August 2024

Table 1
Primers used for bcSRP54 gene clone and functional experiments.

Primer name	Sequence (5′–3′)	Primer information
ORF		ORF cloning
bcSRP54-F	ATGGTTTTAGCTGATCTGGGGAG	
bcSRP54-R	TCACATATTGTTAAATCCCATCATG	
Expression construct		pcDNA5/FRT/To-bcSRP54-Flag
bcSRP54-F(C)	ACTGACGGTACCGCCACCATGGTTTTAGCTGATC	
bcSRP54-R(C)	ACTGACCTCGAGCATATTGTTAAATCCCATCATG	
q-PCR		in vitro q-PCR
bc-Qactin-F	TGGGCACCGCTGCTTCCT	
bc-Qactin-R	TGTCCGTCAGGCAGCTCAT	
bc-QSRP54-F	GGCAGTGGGAAAACCACAAC	
bc-QSRP54-R	ACCTGCTCTGAATGTGTCGG	
shRNA oligos		
sh1-bcSRP54-F	CCGGTCATCAATGAGGAGGTATTAACTCGAGTTAATACCTCCTCATTGATGATTTTTG	shRNA
sh1-bcSRP54-R	AATTCAAAAATCATCAATGAGGAGGTATTAACTCGAGTTAATACCTCCTCATTGATGA	
sh2-bcSRP54-F	CCGGATGTTCTAAGTTGGCATATTACTCGAGTAATATGCCAACTTAGAACATTTTTTG	shRNA
sh2-bcSRP54-R	AATTCAAAAAATGTTCTAAGTTGGCATATTACTCGAGTAATATGCCAACTTAGAACAT	
sh3-bcSRP54-F	CCGGGAAAGGCATGATGGGATTTAACTCGAGTTAAATCCCATCATGCCTTTCTTTTTG	shRNA
sh3-bcSRP54-R	AATTCAAAAAGAAAGGCATGATGGGATTTAACTCGAGTTAAATCCCATCATGCCTTTC	

viral RNA and activate the mitochondrial junction molecule MAVS, which recruits TRAF family proteins or IKK to complete the signal transduction and activate IRF3, IRF7, or NF-κB transcription factors to initiate the transcription and expression of the corresponding genes (Gong et al., 2022). After infection with RNA viruses such as grass carp reovirus (GCRV) or spring viremia of carp virus (SVCV), fish produce interferon (IFN) and establish an antiviral state, highlighting the existence of an IFN antiviral innate immune response in fish (Zhang et al., 2007; Wu et al., 2018). However, studies related to antiviral innate immunity in fish are not sufficiently advanced compared to mammals.

SRP is a complex of RNA and protein that provides a conserved mechanism for the transport of proteins by recognizing hydrophobic sequences on the N-terminus of the proteins to be transported (Doudna and Batey, 2004). Among them, SRP54 plus its binding protein, which plays a key role in the function of the whole SRP, directly binds to the signaling sequences of the initial secretory organ and membrane proteins (Luirink, 2004). However, the role of SRP54 is not limited to directing protein translocation; it also plays a crucial role in a wide range of biological processes. SRP54 plays a role in granulocyte proliferation and differentiation, neutrophil migration capacity and pancreatic exocrine development (Carapito et al., 2017). Recent studies have shown that anti-SRP (in the majority of SRP54) and HMGCR autoantibodies are significant biomarkers in immune-mediated necrotic myopathy (IMNM) (Watanabe et al., 2016). In addition, it has been shown that signal recognition particle 54 (SRP54) acts as a negative regulator of antiviral signal transduction induced by RLRs (Wang, 2021). Over-expression of SRP54 inhibits RNA virus-triggered IFN-β induction and increases viral replication, whereas knockdown of SRP54 produces the opposite effect (Wang, 2021). In fish, it has been reported that the mRNA expression of the immune-associated protein SRP54 is dramatically up-regulated and reaches a maximum at 12 h during *Edwardsiella ictaluri* infection in dark barbel catfish (Li et al., 2019). Studies have also used SRP54 knockout zebrafish as the first *in vivo* model of SRP54 deficiency, indicating that embryonic lethality occurs in SRP54$^{-/-}$ zebrafish and exhibits multiple developmental defects and severe neutropenia (Schürch et al., 2021). These studies demonstrate that SRP54 also exerts immune-related functions in fish. However, the specific function played by SRP54 in the antiviral immune response in fish, as well as the mechanism is unknown.

In the present study, we found that bcSRP54, like mammals, is a negative regulator of RLRs-mediated signaling pathways. Over-expression of bcSRP54 increased the transcription of SVCV-associated genes and decreased the transcript levels of interferon and some antiviral genes, whereas knockdown of bcSRP54 yielded an opposite outcome. Mechanistically, SRP54 interacts with MDA5 and prevents the association of MDA5 with MAVS. The findings of this study indicate that SRP54 plays a novel role in the antiviral innate immune response in fish.

2. Materials and methods

2.1. Cells, plasmids, antibodies, and virus

EPC (*Epithelioma papulosum cyprini* cell line) cells, *M.piceus* kidney (MPK) cells, and HEK-293T cells were kept in the lab and maintained as the reference (Liu et al., 2022).

SVCV (strain: SVCV741) was prepared in EPC cells. Virus infection and titer determination as previously described (Liu et al., 2022). EPC cells transfected with different plasmids were infected with SVCV at different MOI (0.01; 0.1; 1). After a certain period of time, the supernatant was collected, which was serially diluted in a 10-fold gradient and used to infect EPC cells at 26 °C for 2 h, then the supernatant was then discarded and replaced with the DMEM solution containing 1% methylcellulose and 2% FBS and counted virus plaques after 2–3 days. Three replicates were set up for each group to calculate the viral titer. The SVCV titer used for the experiments in this article was 6×10^7 pfu/ml.

pcDNA5/FRT/TO (Thermo Fisher Scientific), pcDNA5/FRT/TO- HA-bcMDA5, pcDNA5/FRT/TO-Myc-bcMAVS, pRL-TK (Avantor), the two types of type-I IFNs, Luci-DrIFNϕ1 (for assessing the transcriptional activity of the zebrafish IFN1 promoter) and Luci-bcIFNa (for assessing the transcriptional activity of black carp IFNa promoter) and PLKO.1-TRC (Addgene) have been kept in the laboratory. Antibodies used in the experiments were obtained from Thermo Fisher Scientific.

2.2. Cloning the CDS of bcSRP54

Regarding the cloning of the bcSRP54 coding regions (CDS), the primers (for the construction of CDS cloning plasmids and expression plasmids, Table 1) were designed based on the prediction full-length transcriptome sequence of black carp. The CDS of black carp SRP54 was cloned from the cDNA of black carp kidney. The cloned fragments were subjected to gel electrophoresis and purified, then inserted into the cloning vector pMD18-T (Thermo Fisher Scientific). The cloned vector constructed was amplified in *Escherichia coil* and purified (small extraction kit), and the purified product was sequenced (TSINGKE). After the sequencing result was correct, the purified product was used as the template for amplification with bcSRP54 expression vector primers (Table 1), and the amplified product was double-digested by restriction endonuclease (KpnI and XhoI). After purification again, the purified product was ligated to pcDNA5/FRT/TO with the Flag label on the C-terminus. The plasmid pcDNA5/FRT/TO-bcSRP54-Flag was used for other experiments.

2.3. Sequence alignment and phylogenetic tree construction

The protein molecular mass and isoelectric point of bcSRP54 were predicted on the EXPASy website (https://web.expasy.org/compute_pi/). MEGA7 was used for multi-sequence comparison, and the comparison result was edited using ESPript 3.0 website (https://espript.ibcp.fr/ESPript/cgi-bin/ESPript.cgi). The protein structural domains of bcSRP54 were predicted using the SMART (https://smart.embl.de/smart/set_mode.cgi?NORMAL=1) online tool. The sequences of the SRP54 protein of all species were saved in a file using the FASTA format. MEGA software aligned the sequences, and a phylogenetic tree was constructed using the neighbor-joining method. The protein 3D structures of bcSRP54 and human SRP54 (hSRP54) were predicted by SWISS-MODEL (https://swissmodel.expasy.org/) online tool.

2.4. Reporter assay

In order to study the effect of bcSRP54 interacting with bcMDA5 on IFN promoter transcription, EPC cells were inoculated into 24-well plates. 16 h later, the reporter plasmid pRL-TK (50 ng), Luci-DrIFNϕ1 (150 ng)/Luci-bcIFNa (150 ng), pcDNA5/FRT/TO-HA-bcMDA5 (40 ng)/empty vector and pcDNA5/FRT/TO- bcSRP54-Flag (0/120 ng/240 ng/360 ng) were transfected (Empty vector were used to make up so that the total amount of transfected plasmid was in the range of 500 ng). Twenty-four hours following transfection, cells were harvested for the dual-luciferase reporter assay (Promega). The measurement method was referred to in our previous paper (Chen, 2021). Briefly, the medium was carefully removed from the 24-well plate, and the wells were washed once with PBS. Then, 100 μl of Passive Lysis Buffer (PLB) was added to each well. The plate was placed in an ice box on a shaker for 15 min to lyse the cells. After mixing the lysate by tapping on the side of the plate, 20 μl of cell lysate from each well was transferred to a 96-well white opaque plate (OptiPlateTM-96, Revvity), and 20 μl of Luciferase Assay Reagent was immediately added to measure Firefly Luciferase activity. After recording the Firefly luminescence, the Renilla Luciferase activity was determined by adding 20 μl of Stop & Glo Reagent and measuring luminescence again. Finally, exporting the data for analysis. Each experiment was repeated three times. All data were normalized against internal references.

2.5. RNA extraction and qPCR assay

Extraction of RNA: Total mRNA extraction for each sample was performed using the HiPure Total RNA Kit from Magen. The PrimeScript™ RT Reagent Kit with gDNA Eraser (Perfect Real Time) (Code No. RR047A) from Takara Bio was used to reverse transcribe the extracted RNA.

Real-time quantitative PCR (qPCR) was performed with SYBR Green® PCR Master Mix (Bio-Rad) to detect the transcript levels of SVCV-associated proteins as well as antiviral genes in EPC cells stimulated with SVCV after overexpression of bcSRP54 or in MPK cells after knockdown the endogenous expression of bcSRP54. The β-actin gene was used as an internal reference for qPCR, and the primer sequences are detailed in Table 1 qPCR procedures were carried out at 95 °C/10 min (1 cycle), 95 °C/15 s, and 60 °C/1 min (35 cycles). Then, dissociation curve analysis (60°C–95 °C) was performed to verify that the amplification was of a single product. The $2^{-\Delta\Delta CT}$ calculation was utilized to determine the relative expression of each gene.

2.6. Immunoblotting

To confirm the correct expression of the bcSRP54 vectors, HEK-293T or EPC cells were inoculated in a six-well plate. Transfection was performed with pcDNA5/FRT/TO-bcSRP54-Flag (3 μg per well) or empty vector (3 μg per well). The expression of bcSRP54 was detected by Western blot. To test for the knockdown effect of bcSRP54, plasmids expressing bcSRP54 and bcSRP54 shRNA or Scramble shRNA were used to co-transfect into HEK-293T cells. The knockdown efficiency of bcSRP54 shRNA was analyzed by ImageJ on the stripes displayed by the Western blot. In a previous paper, the methods for immunoblotting have been thoroughly explained (Wang et al., 2021). Briefly, cell samples were washed three times with PBS and harvested. Next, the cells were centrifuged, the supernatant was removed and then boiled in protein loading buffer for sodium dodecyl sulfate-polyacrylamide gel electrophoresis (SDS-PAGE). Subsequently, the proteins were transferred to polyvinylidene fluoride (PVDF) membranes, blocked with 5% skim milk in TBS for 1 h. The membranes were then incubated with the primary antibody at 4 °C, followed by treatment with an alkaline phosphatase (AP)-coupled secondary antibody. The protein bands were visualized using AP substrate solution (NBT/BCIP). All expression results were standardized with internal references and compared with the control.

2.7. Immunofluorescence

To explore the subcellular location of bcSRP54 in cells, HeLa was inoculated into 24-well plates, transfected with pcDNA5/FRT/TO-bcSRP54-Flag (250 ng) or empty vector (250 ng), and immunofluorescence assay was performed 24 h later. The 24-well plate needs to undergo a round coverslip laying operation before inoculating cells. The method of immunofluorescence was referred to in the previous paper (Wang et al., 2021). Briefly, cells were fixed with 4% paraformaldehyde for 15 min, then permeabilized with 0.2% Triton X-100 for 15 min, and closed with 10% FBS (PBS and fetal bovine serum) for 1 h. Next, cells were incubated with murine monoclonal anti-Flag antibody (1:500) for 1–2 h, followed by incubation with secondary M 488-coupled anti-mouse antibody at a ratio of 1:1000 (this requires protection from light) ratio (light protection is required here). Note that the above steps are followed by washing the cells with PBS before each next step. 8 μl of DAPI (Sigma) was added to the slide for staining the nuclei, and the side of the round coverslip with the cells on it was placed face down on the slide and finally, the edges were sealed to fix the round coverslip. The images were captured with a laser scanning confocal microscope (Olympus FV1200, Japan).

In addition, to investigate whether bcSRP54 co-locates with bcMDA5, the above cells were transfected with pcDNA5/FRT/TO-bcSRP54-Flag (250 ng) and bcMDA5 (250 ng). The subsequent operations were the same as above, with the difference that rabbit monoclonal anti-HA antibody (1:500), as well as R594-coupled anti-rabbit antibody (1:1000), also needed to be added when incubating the antibodies.

2.8. Co-immunoprecipitation (Co-IP)

The interaction between bcSRP54 and bcMDA5 was demonstrated by co-immunoprecipitation. bcSRP54-Flag (7.5 μg) and empty vector (7.5 μg) or bcSRP54-Flag (7.5 μg) and HA-bcMDA5 (7.5 μg) were transfected into HEK-293T in a 10 cm Petri dish. The cells were harvested after transfection for 48 h. After the harvested cells were cleaned, 1 ml 1% NP40 buffer and 10 μl protease inhibitor (1/100 dilution) were added to lyse the cells. The whole cell lysate (WCL) was put on ice for ultrasonic crushing (40W power; crushing 3s, stopping 7s; crushing: total crushing 2 min 30s). After the ultrasonic crushing was completed, the pyrolysis was rotated in a microcentrifuge at a speed of 12000-15000 rpm at 4 °C for 5–10 min, and then 120 μl supernatant was taken as input. Transfer the remaining supernatant to a 1.5 ml ep tube with protein A/G agarose beads, and then rotate on the rotor for 1–2 h at 4 °C to remove the non-specific binding proteins. After 1–2 h, the samples were removed from the rotor and centrifuged at 5000 rpm at 4 °C for 2 min; the supernatant part was taken, and the anti-Flag/HA agarose beads were added to it and incubated at 4 °C for 4–6 h. The anti-Flag/HA agarose beads were cleaned with 1% NP40 buffer 5 times—centrifuge at 5000 rpm at 4 °C for 1 min each time. Finally, add 1 × SDS loading buffer and boil for IB.

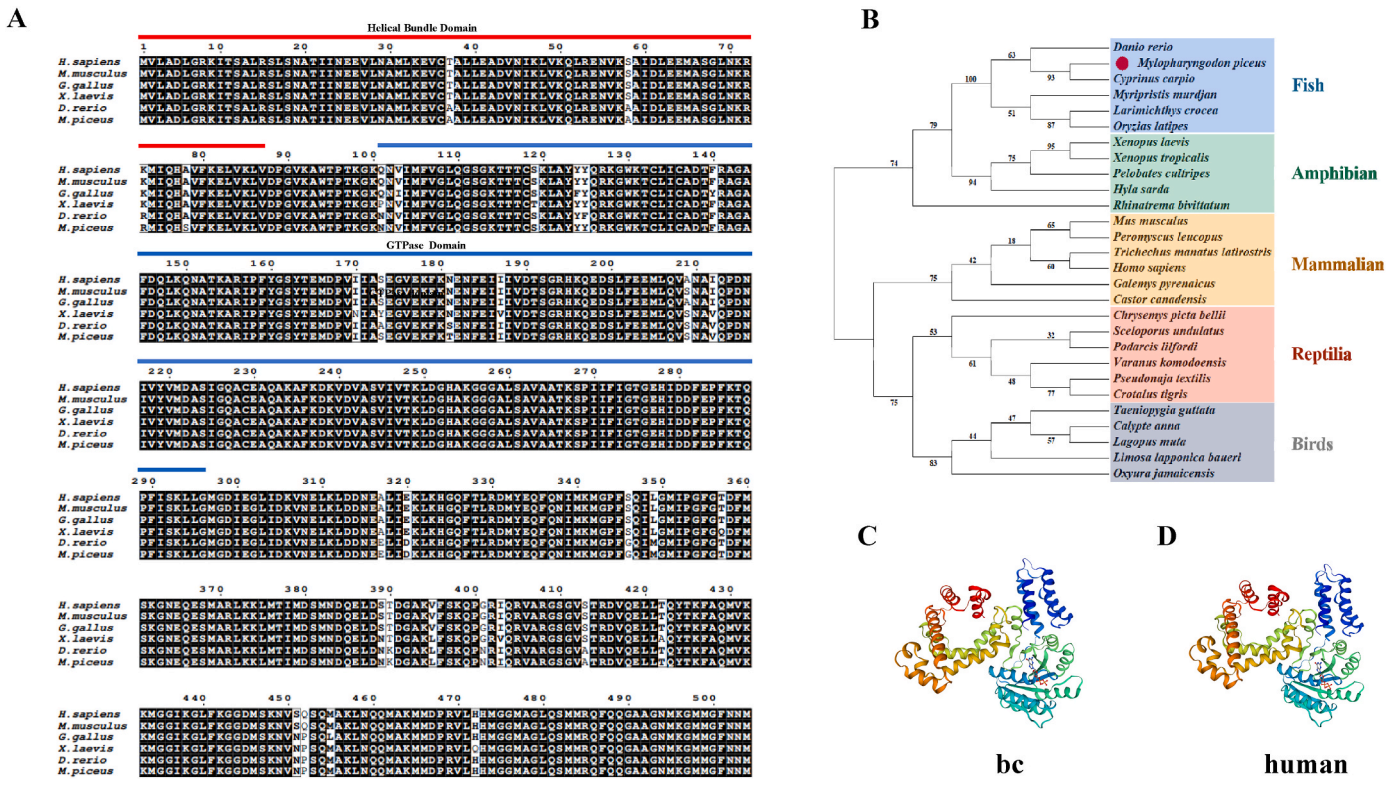

Fig. 1. Sequence alignment, phylogenetic tree analysis, and structure prediction of bcSRP54.
(**A**): The amino acid sequences of the SRP54 gene from *Mylopharyngodon piceus*, *Homo sapiens* (AAC50994.1), *Mus musculus* (NP_001093579.1), *Gallus gallus* (XP_040529991.1), *Xenopus laevis* (XP_018086641.1), and *Danio rerio* (NP_957282.1) were subjected to a multiple sequence alignment. (**B**): Phylogenetic tree generated by different species of the vertebrate SRP54, including: *Mylopharyngodon piceus*, *Danio rerio* (NP_957282.1), *Cyprinus carpio* (XP_042599158.1), *Myripristis murdjan* (XP_029900016.1), *Larimichthys crocea* (XP_010754152.1), *Oryzias latipes* (XP_023807435.1), *Xenopus laevis* (XP_018086641.1), *Xenopus tropicalis* (NP_988977.1), *Pelobates cultripes* (CAH2328366.1), *Hyla sarda* (XP_056401283.1), *Rhinatrema bivittatum* (XP_029454813.1), *Mus musculus* (NP_001093579.1), *Peromyscus leucopus* (XP_028725551.1), *Trichechus manatus latirostris* (XP_004376574.1), *Homo sapiens* (AAC50994.1), *Galemys pyrenaicus* (KAG8516459.1), *Castor canadensis* (XP_020036303.1), *Chrysemys picta bellii* (XP_008162511.1), *Sceloporus undulatus* (XP_042311903.1), *Podarcis lilfordi* (CAI5764164.1), *Varanus komodoensis* (XP_044292090.1), *Pseudonaja textilis* (XP_026566858.1), *Crotalus tigris* (XP_039207769.1), *Taeniopygia guttata* (XP_002200552.1), *Calypte anna* (KFO97182.1), *Lagopus muta* (XP_048803319.1), *Limosa lapponica baueri* (PKU44966.1), *Oxyura jamaicensis* (XP_035185157.1). (**C-D**): Comparison of predicted 3D protein structures of bcSRP54 and human SRP54 using the online tool SWISS-MODEL.

2.9. Virus infection and titre

To detect the effect of bcSRP54 interaction with bcMDA5 on the antiviral ability of cells, EPC cells were inoculated in 24-well plates. After 16 h inoculation, transfected empty vector (500 ng), bcSRP54 (450 ng) and empty vector (50 ng), bcMDA5 (50 ng) and empty vector (450 ng), or bcSRP54 (450 ng) and bcMDA5 (50 ng). After transfection for 24 h, 500 μl DMEM was exchanged per well, which contained the specified amount of SVCV. After SVCV infection for 1–2 h, cells were cleaned with PBS and added to 500 μl DMEM medium containing 2% FBS. After 24 h, the supernatant was collected to the determination of viral titer. Viral titers were assayed as described in 2.1.

To test the effect of knockdown of bcSRP54 on host cells' antiviral resistance, MPK cells were transfected with either the bcSRP54 shRNA plasmid or the Scramble shRNA plasmid. Viral infection and titer experiments were the same as above.

2.10. bcSRP54 shRNA design

The bcSRP54 shRNA oligonucleotides (Table 1) were designed on the GPP Web Portal (https://portals.broadinstitute.org/gpp/public/seq/search) website. After the design was completed, three pairs of oligonucleotides (Table 1) were selected for the synthesis of bcSRP54 shRNA and sent the sequences to the company (TSINGKE) for synthesis. After getting the primer sample, the annealing experiment was carried out. PLKO-shRNA-bcSRP54-1 (sh-1), PLKO-shRNA-bcSRP54-2 (sh-2), and PLKO- shRNA-bcSRP54-3 (sh-3) oligonucleotides were inserted into PLKO.1-TRC plasmid to form three knockdown plasmids of bcSRP54. The synthesized primers (20 μM) were combined with 5 μl forward primers and 5 μl reverse primers, 5 μl 10 × NEB PCR buffer, and 35 μl ddH_2O to form a 50 μl annealing system. The annealing procedure was 95 °C for 5 min, and then the samples were placed in 95 °C water and cooled to room temperature. The annealing product is a double-stranded oligonucleotide, which needs to be inserted into PLKO.1-TCR. PLKO.1 was first double-digested with restriction enzymes EcoRI and AgeI, purified after digestion, and then ligated with the double-stranded oligonucleotides by T4 DNA ligase (Vazama, China). The knockdown plasmid of bcSRP54 was transformed, batched, and shaken, and finally, the extracted plasmid was sent to the company (TSINGKE) for sequencing.

2.11. Statistic analysis

All statistical analyses, including qPCR, luciferase reporter assay, and viral titers, were averaged from three parallel experiments. All bar graphs were created using GraphPad Prism 8 (GraphPad Software, San Diego, USA). The STDEVP function calculates the value of the error line. The data were analyzed using a Two-tailed Student's t-test. The asterisk * represents $p < 0.05$, ** represents $p < 0.01$, *** represents $p < 0.001$, and **** represents $p < 0.0001$.

Table 2
Comparison of bcSRP54 with other vertebrate SRP54 (%).

Species	Full-length sequence of protein	
	Identity	Similarity
Mylopharyngodon piceus	100	100
Danio rerio	99.21	100
Cyprinus carpio	99.60	99.80
Myripristis murdjan	99.01	99.80
Larimichthys crocea	98.21	99.80
Oryzias latipes	98.61	99.80
Xenopus laevis	95.83	97.62
Xenopus tropicalis	95.83	97.62
Pelobates cultripes	96.23	97.62
Hyla sarda	96.03	97.62
Rhinatrema bivittatum	96.23	98.61
Mus musculus	96.43	98.41
Peromyscus leucopus	96.23	98.41
Trichechus manatus latirostris	96.03	98.21
Homo sapiens	96.23	98.41
Galemys pyrenaicus	96.22	98.41
Castor canadensis	96.03	98.41
Chrysemys picta bellii	96.23	98.61
Sceloporus undulatus	95.63	98.61
Podarcis lilfordi	95.69	98.36
Varanus komodoensis	95.83	98.61
Pseudonaja textilis	95.44	98.61
Crotalus tigris	95.44	98.41
Taeniopygia guttata	95.83	98.61
Calypte anna	95.63	98.61
Lagopus muta	95.63	98.41
Limosa lapponica baueri	95.63	98.61
Castor canadensis	96.03	98.41
Oxyura jamaicensis	96.03	98.81

3. Results

3.1. Sequence analysis of bcSRP54

Sequencing results showed that bcSRP54 comprises 1515 nucleotides that encode 504 amino acids. The protein sequences of SRP54 from human (*Homo sapiens*), mouse (*Mus musculus)*, bird (*Gallus gallus*), frog (*Xenopus laevis*) and fish (*Danio rerio*) were downloaded from NCBI and compared with black carp in a multiple sequence comparison, which showed that SRP54 is very evolutionarily conserved in vertebrate (Fig. 1A), with the highest degree of similarity to *Danio rerio* at 100% (Table 2). The protein sequence of bcSRP54 was subjected to structural domain prediction on SMART, where amino acids 2–87 are helix bundle structural domains and amino acids 101–296 are GTPase structural domains (Fig. 1A). To further understand the evolutionary relationships of bcSRP54 in vertebrates, we also constructed an evolutionary tree with 28 species selected from different categories, including fish, amphibians, mammals, reptiles, and birds. The similarity and identity of SRP54 amino acid sequence between black carp and the species in the evolutionary tree are shown in Table 2. The results showed that common carp and black carp SRP54 were the most closely related (Fig. 1B). The three-dimensional constructions of bcSRP54 and human SRP54 were compared by SWISS-MODEL, the results indicate that SRP54 is highly conserved in structure (Fig. 1C and D).

3.2. The protein expression of bcSRP54 and its cellular location

The predicted molecular mass of bcSRP54's amino acid sequence is 55.8 kDa, with an isoelectric point of 8.87. (EXPASy Compute PI/Ww calculation). Western blot results showed that bands of bcSRP54 overexpression in HEK-293T and EPC cells were approximately 55 kDa, consistent with the predicted results (Fig. 2A and B). Immunofluorescence experiments of overexpression of bcSRP54 in HeLa cells demonstrated that the green fluorescence was primarily distributed within the cytoplasm (Fig. 2C). In summary, bcSRP54 can be expressed in both HEK-293T and EPC cells, and is mainly localized in the cytoplasm.

3.3. bcSRP54 depresses bcMDA5-activated IFN promoter transcription

Previous studies have shown that SRP54 interacts with MDA5 to negatively regulate the antiviral innate immune response (Wang, 2021). This study examined the effect of bcSRP54 on the transcription of bcMDA5-activated IFN promoter. The results indicate that bcSRP54 down-regulates bcIFNa and DrIFNϕ1 promoter activities upon co-transformation with MDA5 and acts on bcMDA5 in a dose-dependent manner (Fig. 3A and B). Experimental results showed that MDA5-mediated activities of bcIFNa and DrIFNϕ1 promoters gradually

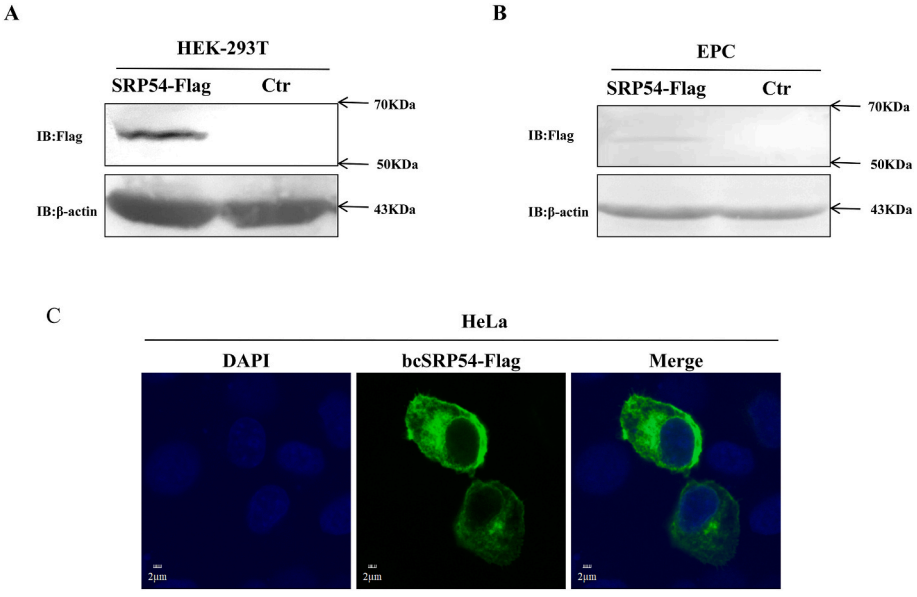

Fig. 2. The protein expression of bcSRP54.
(**A-B**): Expression of bcSRP54-Flag plasmid was detected by immunoblotting assay using HEK-293T cells (A) and EPC cells (B). IB: immunoblot. (**C**): HeLa cells were transfected with the plasmid of bcSRP54-Flag in 24-well plates and immunofluorescence staining was performed to detect its location in the cells according to the method. bcSRP54-Flag: pcDNA5/FRT/TO-bcSRP54-Flag; Ctr: pcDNA5/FRT/TO; The scale represents 2 μm.

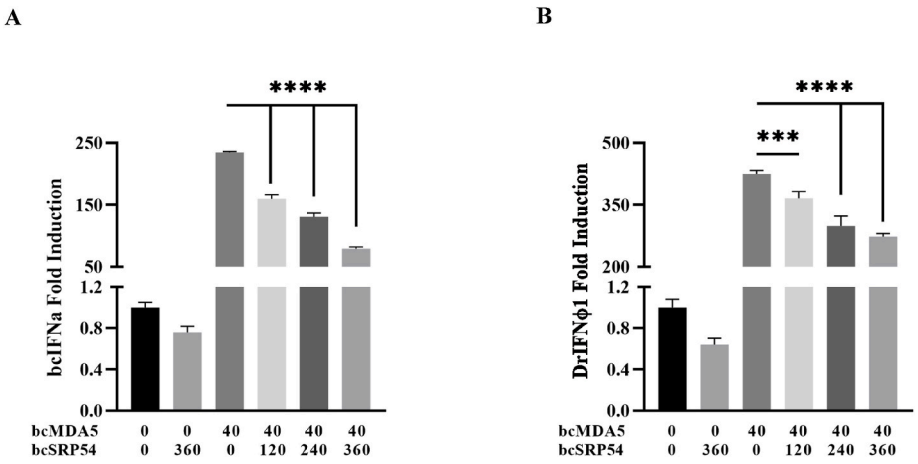

Fig. 3. bcSRP54 inhibits MDA5-mediated interferon production.
(**A-B**): EPC cells were transfected with different doses of plasmids (unit: ng) shown in the figure, reporter plasmids Luci-bcIFNa (A)/Luci-DrIFNϕ1 (B) and pRL-TK. Then, the luciferase reporter assay definitively detected the transcriptional activities of the two promoters. bcSRP54: pcDNA5/FRT/TO-bcSRP54-Flag; bcMDA5: pcDNA5/FRT/TO-HA-bcMDA5; Ctr: pcDNA5/FRT/TO. *P < 0.05, **P < 0.01.

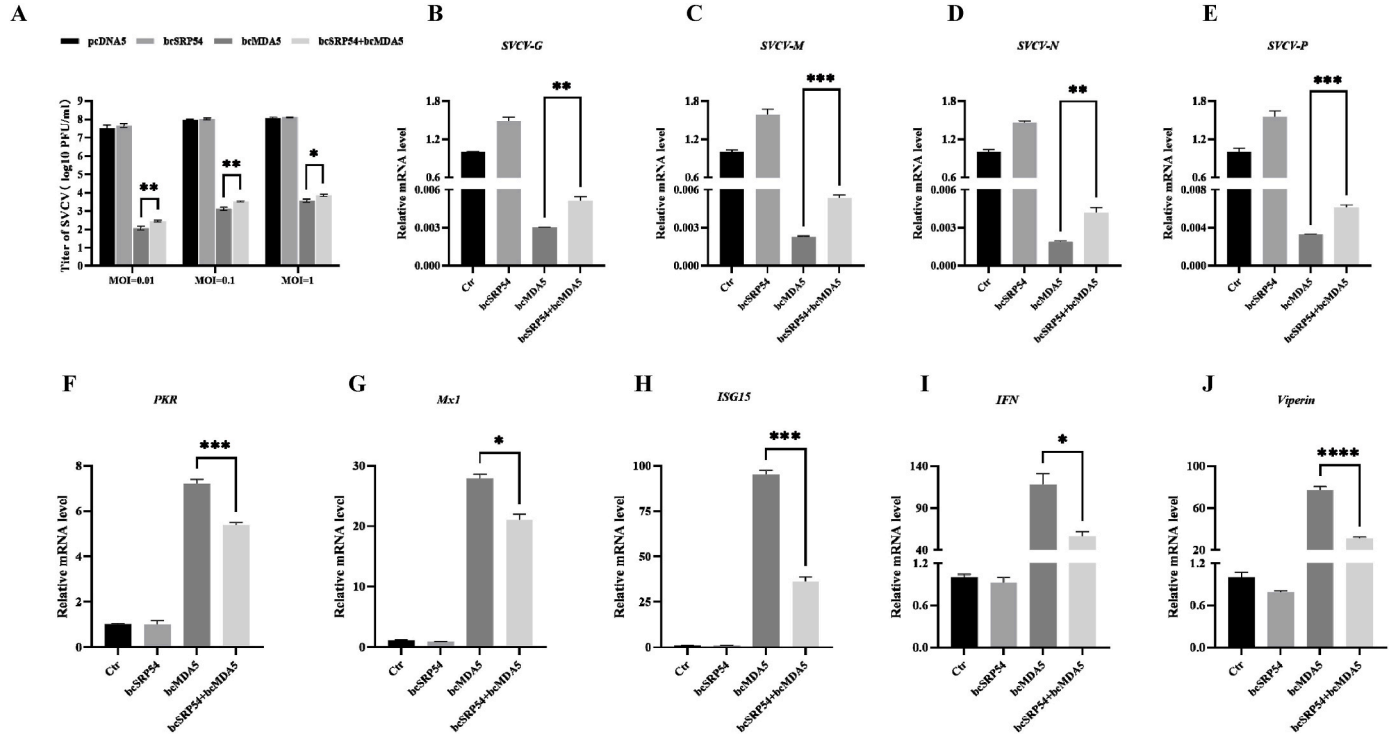

Fig. 4. Over-expression of bcSRP54 inhibits the antiviral activity of bcMDA5.
(**A**): EPC cells were transfected with plasmids expressing bcSRP54 and bcMDA5 in 24-well plates, and then SVCV infection was performed for 24 h. The supernatant was collected 24 h after virus infection, and the viral titer in the supernatant was determined by plaque assay. (**B-E**): EPC cells were transfected with bcSRP54, bcMDA5 individually or co-transfected with bcSRP54 and bcMDA5 in 24-well plates. 24 h later, the cells were infected with SVCV (MOI = 0.01), and RNA was extracted 24 h after viral infection. Virus-free treatment group as control. *SVCV-G*, *M*, *N*, and *P* mRNA expression levels were detected using qPCR. (**F-J**): EPC cells were transfected with bcSRP54, bcMDA5 alone or bcSRP54 and bcMDA5 together in 12-well plates. 24 h later, cells were infected with SVCV (MOI = 0.1), and RNA was extracted at 6 h after viral infection. Virus-free treatment group as control. qPCR was carried out to measure the mRNA expression levels of each group of *epcPKR*, *epcMX1*, *epcISG15*, *epcIFN*, and *epcViperin*. bcSRP54: pcDNA5/FRT/TO- bcSRP54-Flag; bcMDA5: pcDNA5/FRT/TO-HA-bcMDA5; Ctr: pcDNA5/FRT/TO. *P < 0.05, **P < 0.01.

decreased with increasing doses of bcSRP54. All these data suggest that bcSRP54 negatively regulates bcMDA5-mediated IFN signaling.

3.4. bcSRP54 inhibits bcMDA5-mefiated antiviral ability

Our data showed that bcSRP54 negatively regulates the transcriptional activity of bcMDA5-activated IFN promoter. We therefore further explored the effect of bcSRP54 on bcMDA5-mediated antiviral resistance. The plaque assay results showed that in EPC cells, overexpression of bcMDA5 significantly decreased the viral titer of the supernatant medium compared with the control group transfected with empty vector. When bcSRP54 was co-transferred with bcMDA5, the viral

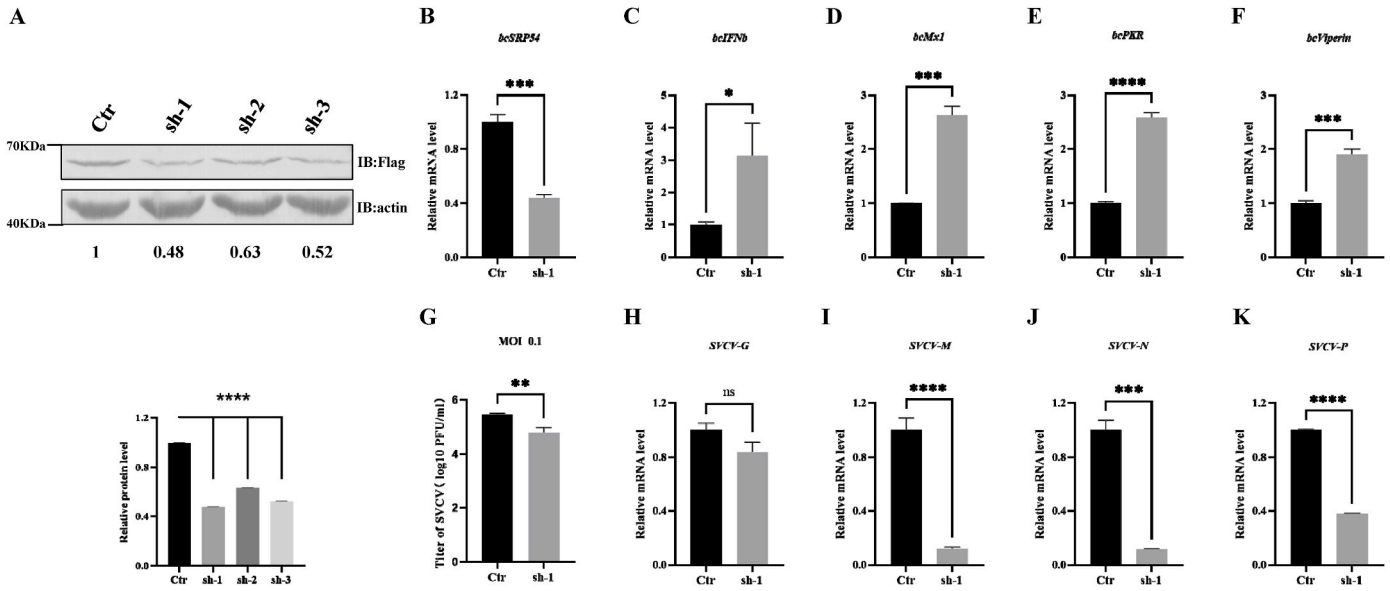

Fig. 5. Interfering with the expression of bcSRP54 enhances the antiviral capacity of MPK cells.
(**A**): HEK-293T cells were co-transfected with bcSRP54 (1.5 μg) and each of the shRNAs, sh-1, sh-2 and sh-3 (each at 1.5 μg) in 6-well plates. Using scramble as a control group. And the expression levels of bcSRP54 were detected by immunoblotting. Protein expression levels of bcSRP54 were quantified by ImageJ software through greyscale analysis. (**B**): MPK cells were transfected with either scrambled control or sh-1 in 12-well plates, and the endogenous mRNA levels of bcSRP54 were quantified by qPCR. (**C-F**): MPK cells were transfected with scramble or sh-1, and the mRNA expression levels of *bcIFNb*, *bcMX1*, *bcPKR,* and *bcViperine* were detected by qPCR 24 h later. (**G**) MPK cells with knockdown of SRP54 were infected with SVCV at MOI = 0.1 in a 24-well plate, and the supernatant was collected 24 h later for viral titer assay. (**H-K**): MPK cells transfected with scramble or sh-1 were infected with SVCV at 0.1 MOI for 24 h. The mRNA expression levels of *SVCV-G*, *M*, *N,* and *P* were detected by qPCR. bcSRP54: pcDNA5/FRT/TO-bcSRP54-Flag; sh-1: PLKO-shRNA-bcSRP54-1; sh-2: PLKO-shRNA-bcSRP54-2; sh-3: PLKO-shRNA-bcSRP54-3; Scramble: PLKO-shRNA-scramble. *P < 0.05, **P < 0.01.

titer was significantly increased compared with in the group singly expressed with bcMDA5 (Fig. 4A). This indicated that overexpression of bcMDA5 limited SVCV replication in EPC cells, while co-expressing bcSRP54 decreased bcMDA5 mediated antiviral ability. To further validate this result, we checked the expression levels of SVCV viral proteins, as well as downstream antiviral proteins in the above groups of EPC cells that infected with SVCV at MOI = 0.1. The results indicated that bcSRP54 increased transcript levels of *SVCV-G*, *M*, *N*, and *P* and decreased the transcript levels of genes related to the MDA5-mediated IFN signaling pathway (*epcPKR*, *epcMX1*, *epcISG15*, *epcIFN*, *epcViperine*) in EPC cells (Fig. 4B–E and Fig. 4F–J). Taken together, it appears that bcSRP54 has a negative regulatory effect on MDA5-mediated antiviral immune responses.

3.5. Knockdown bcSRP54 results in enhanced antiviral capability

In order to investigate the impact of bcSRP54 on IFN signaling in host cells, we designed shRNA against bcSRP54 and detected knockdown efficiency in HEK-293T. The results showed that sh-1, sh-2, and sh-3 all had knockdown effects, and the sh-1 was the most significant, with the

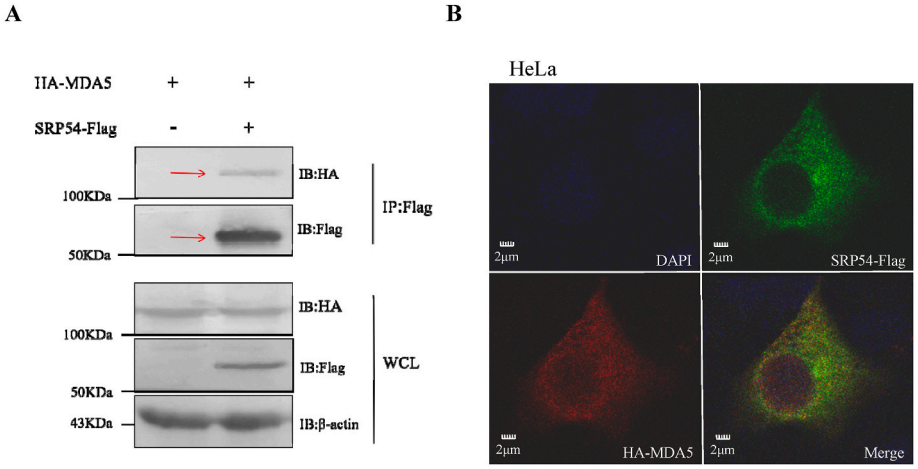

Fig. 6. bcSRP54 interacts with bcMDA5.
(**A**): pcDNA5/FRT/TO-HA-bcMDA5 (7.5 μg) was co-transfected with pcDNA5/FRT/TO-bcSRP54-Flag (7.5 μg) or empty vector (7.5 μg) in HEK-293T cells, and immunoprecipitation (IP) assay after 48 h. IP was performed using bcSRP54 as bait protein. IP: immunoprecipitation; IB: immunoblotting; WCL: whole cell lysate; SRP54-Flag: pcDNA5/FRT/TO- bcSRP54-Flag; HA-MDA5: pcDNA5/FRT/TO-HA-bcMDA5. (**B**): HeLa cells were co-transfected with plasmids expressing bcSRP54-Flag and HA-bcMDA5 and stained for immunofluorescence according to the method. SRP54-Flag: pcDNA5/FRT/TO- bcSRP54-Flag; HA-MDA5: pcDNA5/FRT/TO-HA-bcMDA5; The scale represents 2 μm.

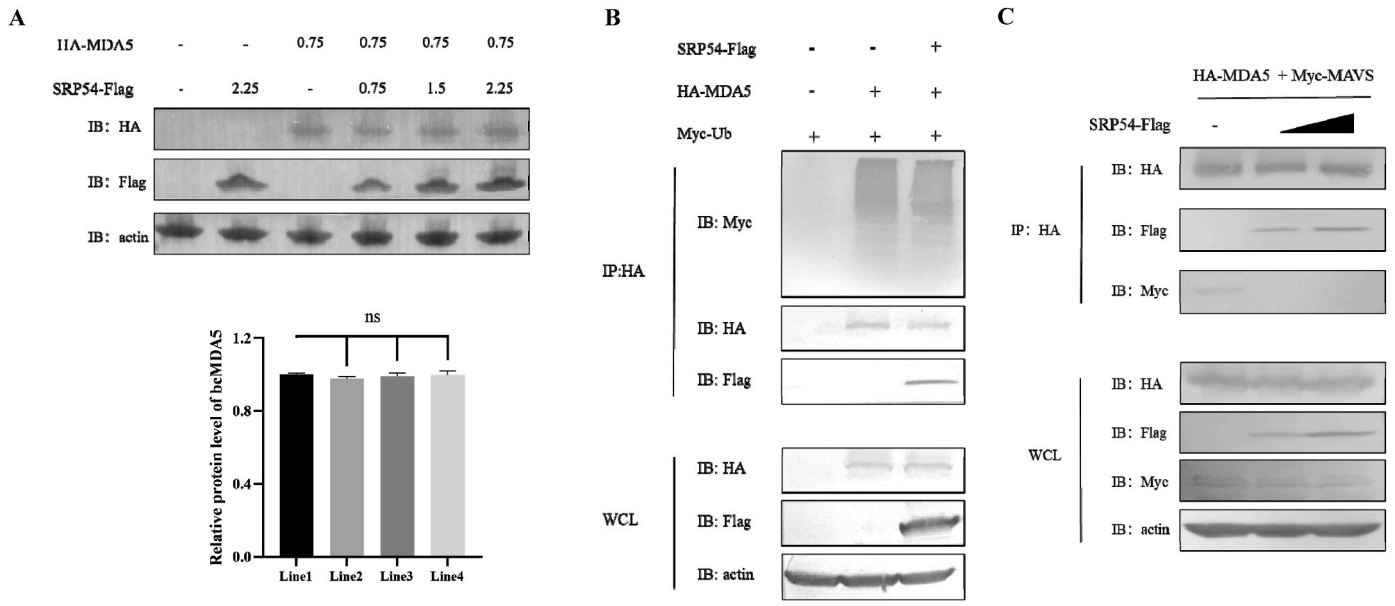

Fig. 7. bcSRP54 hinders the binding of MDA5 to MAVS.
(A): HEK-293T cells were singly transfected with bcSRP54 (2.25 μg) or bcMDA5 (0.75 μg) and co-transfected with bcSRP54 (0.75 μg, 1.5 μg or 2.25 μg) and bcMDA5 (0.75 μg) in 6-well plates. The expression of bcMDA5 was detected by immunoblotting. The protein expression level of bcMDA5 was quantified using ImageJ software. IB: immunoblot. (**B**): 10 cm large dishes HEK-293T cells were transfected with Ub (5 μg), co-transfected with bcMDA5 (5 μg) and Ub (5 μg), and co-transfected with bcSRP54 (5 μg), bcMDA5 (5 μg) and Ub (5 μg). The cells were collected 48 h later and were used for the process of immunoprecipitation (IP). IP was performed using bcMDA5 as bait protein. IP: immunoprecipitation; IB: immunoblotting; WCL: whole cell lysate; SRP54-Flag: pcDNA5/FRT/TO- bcSRP54-Flag; HA-MDA5: pcDNA5/FRT/TO-HA-bcMDA5; Myc-Ub: pcDNA5/FRT/TO-Myc-Ub (**C**): 10 cm large dishes of HEK-293T were co-transfected with bcMDA5 (3 μg), bcMAVS (3 μg) and bcSRP54 (0 μg, 3 μg or 6 μg). The cells were collected 48 h later and were used for the process of immunoprecipitation (IP). The IP was conducted utilizing bcMDA5 as the bait protein. IP: immunoprecipitation; IB: immunoblotting; WCL: whole cell lysate; SRP54-Flag: pcDNA5/FRT/TO-bcSRP54-Flag; HA-MDA5: pcDNA5/FRT/TO-HA-bcMDA5; Myc-MAVS: pcDNA5/FRT/TO-Myc-bcMAVS.

expression of bcSRP54 subtracted about 52% in HEK-293T (Fig. 5A). Therefore, we chose sh-1 for the subsequent experiment. The qPCR results showed that overexpression of sh-1 significantly reduced the mRNA levels of endogenous bcSRP54 in MPK cells and resulted in the promotion of the mRNA transcription levels of *IFNb*, *MX1*, *PKR*, and *Viperine* (Fig. 5B–F). In addition, the subsequently plaque assay showed that viral titers in the supernatant of bcSRP54 knockdown MPK cells were lower than that of controls, and mRNA levels of *M*, *N*, and *P* were also markedly suppressed compared to those of controls (Fig. 5G–K). Together, these data suggest that knocking down bcSRP54 enhances host antiviral resistance, which further suggests that bcSRP54 plays a negative regulatory role in the host antiviral response.

3.6. bcSRP54 interacts with bcMDA5

To verify whether the existence of interaction between bcSRP54 and bcMDA5, immunoprecipitation experiments were carried out. In 293T cells, single transfection of bcMDA5 was used as a control, and co-transfection of bcSRP54 with bcMDA5 was used as an experimental group to explore whether there is an interaction between SRP54 and MDA5. The WB results show that immunoprecipitation with anti-Flag, bring down the Flag-tagged bcSRP54 and the HA-tagged MDA5 from 293T cells co-transfected with bcMDA5 and bcSRP54. The HA-specific MDA5 band in co-transfected cells suggests that there is an interaction between bcSRP54 and bcMDA5 (Fig. 6A). Meanwhile, immunofluorescence results also indicated the co-location between bcSRP54 and MDA5 (Fig. 6B). This is further evidence of an interaction between bcSRP54 and bcMDA5. All this provides a evidence for that SRP54 can influence MDA5-mediated antiviral innate immunity.

3.7. bcSRP54 does not affect the ubiquitination levels of bcMDA5

In order to further investigate in what way bcSRP54 affects the antiviral activity of bcMDA5, we firstly co-transfected bcMDA5 with dose-escalating bcSRP54 in HEK-293T cells, and found that the effect of incremental increase of bcSRP54 had no significant difference on the protein expression level of bcMDA5 (Fig. 7A). Then experiments on total ubiquitination were performed, and the WB results showed that the ubiquitination levels of bcMDA5 did not undergo significant enhancement or decrease when co-expressed with bcSRP54 (Fig. 7B).

3.8. bcSRP54 affects the binding of bcMAVS to bcMDA5

To further investigate the mechanism of negatively regulation role of bcSRP54 on bcMDA5 mediated antiviral signaling, we referred to previous studies and examined whether SRP54 similarly perturbed the recruitment of MAVS by MDA5 in bony fishes. The competitive coimmunoprecipitation experiments results showed that bcSRP54 prevented the binding of bcMDA5 to bcMAVS (Fig. 7C). This further indicates that SRP54 is conserved in sequence in terms of function.

4. Discussion

The structure of a protein is highly linked to its function. Differences in amino acid sequences lead to differences in primary structure, which in turn affect the secondary, tertiary, and quaternary structures of proteins (Alberts et al., 2002). The way a protein folds affects its shape, surface properties, and spatial structure, which determines its function (Chen, 2020). For example, enzymes are specialized proteins whose structure is essential for catalyzing chemical reactions. The active site of an enzyme is closely related to its structure, and it is only in a particular structure that the enzyme can bind to a substrate and catalyze a reaction (Chen, 2020). Besides, the relationship between the structure of a protein and its function is reflected in its specific structural domains (Grützner et al., 2021). Proteins usually consist of multiple structural domains, each with a specific function. For example, immunoglobulins

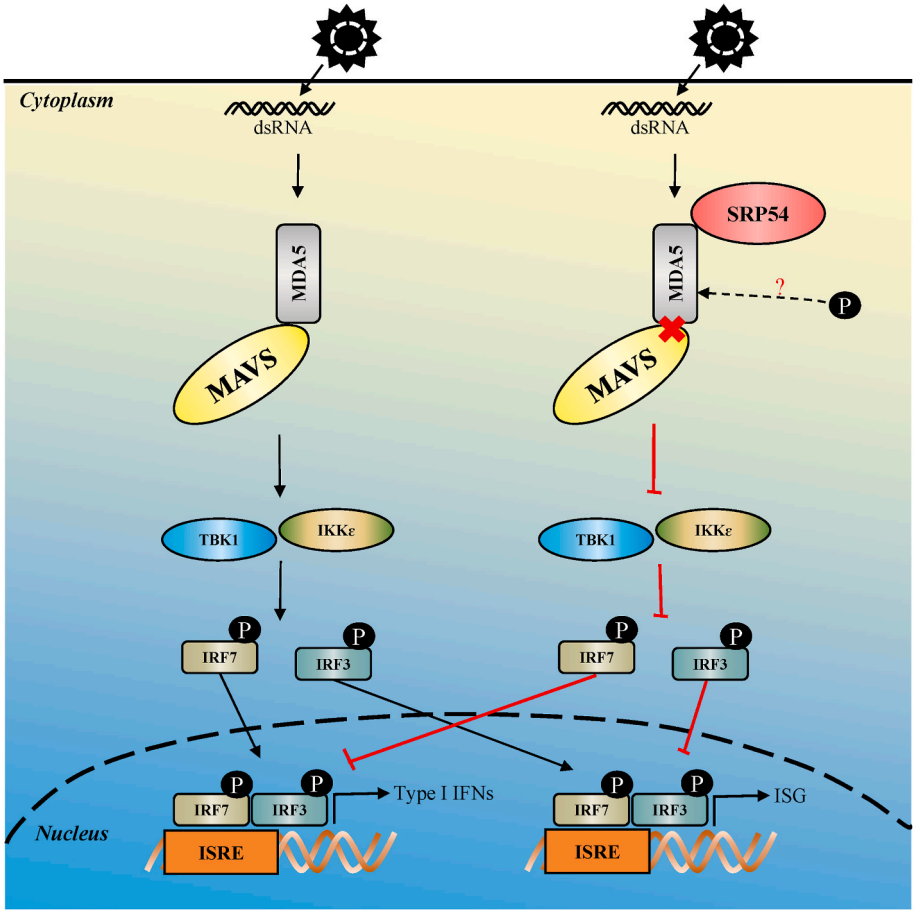

Fig. 8. Summary of black carp SRP54 negatively regulates MDA5-mediated antiviral innate immunity.

are antibodies that consist of an antigen-binding domain and an effector molecule-binding domain, which are responsible for binding antigens and prompting an immune response, respectively (Schroeder and Cavacini, 2010). The presence of such specific structural domains allows proteins to fulfill specific biological functions in the cell.

In this study, the bcSRP54 of black carp was cloned and characteristic. Sequence alignment and evolutionary tree analyses indicate that SRP54 is highly conserved across species in vertebrates. Its three-dimensional structure is also highly similar to humans, which implied we that its biological function might be conservative. It has been shown that in mammals, the structural domain of SRP54 consists of three parts: an N-terminal structural domain (N structural domain), a central GTPase structural domain (G structural domain), which are interlinked in GTP-dependent interactions with SRP receptors on the ER membrane, and a C-terminal M structural domain which binds to RNP 7SL RNA and the signal peptide of the nascent polypeptide (Janda et al., 2010). The predicted structural domain of bcSRP54 is composed of helix bundle structural domains at the N-terminal and GTPase structural domains in the middle. However, the M structural domain at the C-terminal was not identified by SMART analysis. We speculate that this domain is present but not as conserved, which may deserve further study in the future. Since the aim of our study was to examine the role of SRP54 in antiviral innate immunity in fish and the function of bcSRP54 was conserved, we did not go deeper into the conservation of the M structural domain. Recently, SRP54 has been identified as a negative regulator of the innate immune response to RNA viruses (Wang, 2021). In this study, we found that SRP54 plays a similar role in teleost fish. It was identified to play a negative effect on antiviral responses by interacting with bcMDA5 and disrupting the binding of bcMDA5 to bcMAVS. The knockdown of SRP54 in the host cells increases the host cell's antiviral ability. The conserved function of bcSRP54 might be related to its highly conservative protein sequences and structure.

It has been shown that SRP54 can function as an important GTPase during co-translation (Hainzl et al., 2007; Juaire et al., 2021). However, according to reporter gene assays, GTPase-deficient mutants of SRP54, as well as wild-type SRP54, both inhibit RLR signaling, suggesting that this activity is dispensable (Wang, 2021). This suggests that SRP54's inhibitory function on the innate immune response is not mediated by SRP-dependent protein translocation but rather represents a novel function of SRP54. SRP54 is known to function mainly in directing the transport of newly synthesized secreted proteins from polyribosomes to the endoplasmic reticulum (Egea et al., 2005; Zhang et al., 2023). The sites at which its novel functions in antiviral immunity specifically play a role are unknown. In this study, unlike its mammalian counterpart, the bcSRP54 is predicted to lack the classic C-terminal M structural domain, while still playing a similar negative role in RLRs-mediated innate immune response by disrupting the recruitment of MAVS to MDA5 as in mammalian. Considering the innate immune response inhibitory function of SRP54 is not mediated by the GTPase domain as mentioned previously, the results in this study suggest that the antiviral role of SRP might be related to its N-terminal domain.

The N terminus of MDA5 is known to have tandem CARDs domains, which recruit MAVS through CARD-CARD homo interactions and ultimately promote the activation of the type I interferon (IFN) pathway (Li et al., 2023; Song et al., 2021). As shown in the summary diagram (Fig. 8), our study revealed that SRP54 inhibited the binding of MDA5 to MAVS, but the specific mechanism of inhibition is unknown. Whether this is due to the competitive binding of SRP54 and MAVS to the structural domain of CARDs of MDA5 or by affecting the phosphorylation modification of MDA5 needs further experimental verification.

In summary, our study indicates that bcSRP54 negatively regulates MDA5-mediated antiviral innate immunity signaling by disrupting the recruitment of MAVS to MDA5. These discoveries shed light on the role of SRP54 in the innate immune system of bony fishes and offer novel insights into the mechanism of antiviral immunity in fish.

CRediT authorship contribution statement

Jixiang Chu: Writing – original draft, Investigation. **Yixia Chen:** Visualization, Investigation. **Yanfang Wu:** Visualization, Methodology. **Wei Qin:** Investigation. **Jun Yan:** Writing – review & editing, Conceptualization. **Jun Xiao:** Writing – review & editing, Conceptualization. **Hao Feng:** Writing – review & editing.

Declaration of competing interest

All authors declare that they have no conflict of interest.

Data availability

The data that has been used is confidential.

Acknowledgments

This work was supported by the National Natural Science Foundation of China (U21A20268, U22A20535, 31920103016, 32173010), Hunan Provincial Science and Technology Department (2023JJ10010028, 2022JJ30383, 2023JJ40435), the Modern Agricultural Industry Program of Hunan Province, the Research and Development Platform of Fish Disease and Vaccine for Postgraduates in Hunan Province.

References

Alberts, B., Johnson, A., Lewis, J., Raff, M., Roberts, K., Walter, P., 2002. Molecular Biology of the Cell, fourth ed. Garland Science.

Carapito, R., Konantz, M., Paillard, C., Miao, Z., Pichot, A., Leduc, M.S., Yang, Y., Bergstrom, K.L., Mahoney, D.H., Shardy, D.L., Alsaleh, G., Naegely, L., Kolmer, A., Paul, N., Hanauer, A., Rolli, V., Müller, J.S., Alghisi, E., Sauteur, L., Macquin, C., Morlon, A., Sancho, C.S., Amati-Bonneau, P., Procaccio, V., Mosca-Boidron, A.-L., Marle, N., Osmani, N., Lefebvre, O., Goetz, J.G., Unal, S., Akarsu, N.A., Radosavljevic, M., Chenard, M.-P., Rialland, F., Grain, A., Béné, M.-C., Eveillard, M., Vincent, M., Guy, J., Faivre, L., Thauvin-Robinet, C., Thevenon, J., Myers, K., Fleming, M.D., Shimamura, A., Bottollier-Lemallaz, E., Westhof, E., Lengerke, C., Isidor, B., Bahram, S., 2017. Mutations in signal recognition particle SRP54 cause syndromic neutropenia with Shwachman-Diamond–like features. J. Clin. Invest. 127, 4090–4103. https://doi.org/10.1172/JCI92876.

Chen, K., 2020. Engineering new catalytic activities in enzymes. Nat. Catal. 3, 203–213. https://doi.org/10.1038/s41929-019-0385-5.

Chen, Z., 2021. NLK suppresses MAVS-mediated signaling in black carp antiviral innate immunity. Dev. Comp. Immunol. https://doi.org/10.1016/j.dci.2021.104105.

Chunhaphinyokul, B., Hosokai, E., Miyamoto, M., Komuro, A., 2023. Differential regulation of ATP hydrolysis of RIG-I-like receptors by transactivation response RNA-binding protein. Biosci. Rep. 43, BSR20222152 https://doi.org/10.1042/BSR20222152.

Doudna, J.A., Batey, R.T., 2004. Structural insights into the signal recognition particle. Annu. Rev. Biochem. 73, 539–557. https://doi.org/10.1146/annurev.biochem.73.011303.074048.

Duic, I., Tadakuma, H., Harada, Y., Yamaue, R., Deguchi, K., Suzuki, Y., Yoshimura, S.H., Kato, H., Takeyasu, K., Fujita, T., 2020. Viral RNA recognition by LGP2 and MDA5, and activation of signaling through step-by-step conformational changes. Nucleic Acids Res. 48, 11664–11674. https://doi.org/10.1093/nar/gkaa935.

Egea, P.F., Stroud, R.M., Walter, P., 2005. Targeting proteins to membranes: structure of the signal recognition particle. Curr. Opin. Struct. Biol. 15 (2), 213–220. https://doi.org/10.1016/j.sbi.2005.03.007.

Fan, X., Jin, T., 2019. Structures of RIG-I-like receptors and insights into viral RNA sensing. In: Jin, T., Yin, Q. (Eds.), Structural Immunology, Advances in Experimental Medicine and Biology. Springer Singapore, Singapore, pp. 157–188. https://doi.org/10.1007/978-981-13-9367-9_8.

Gong, X.-Y., Zhang, Q.-M., Zhao, X., Li, Y.-L., Qu, Z.-L., Li, Z., Dan, C., Gui, J.-F., Zhang, Y.-B., 2022. LGP2 is essential for zebrafish survival through dual regulation of IFN antiviral response. iScience 25, 104821. https://doi.org/10.1016/j.isci.2022.104821.

Grützner, J., Billenkamp, F., Spanka, D.-T., Rick, T., Monzon, V., Förstner, K.U., Klug, G., 2021. The small DUF1127 protein CcaF1 from *Rhodobacter sphaeroides* is an RNA-binding protein involved in sRNA maturation and RNA turnover. Nucleic Acids Res. 49, 3003–3019. https://doi.org/10.1093/nar/gkab146.

Hainzl, T., Huang, S., Sauer-Eriksson, A.E., 2007. Interaction of signal-recognition particle 54 GTPase domain and signal-recognition particle RNA in the free signal-recognition particle. Proc. Natl. Acad. Sci. U.S.A. 104 (38), 14911–14916. https://doi.org/10.1073/pnas.0702467104.

Janda, C.Y., Li, J., Oubridge, C., Hernández, H., Robinson, C.V., Nagai, K., 2010. Recognition of a signal peptide by the signal recognition particle. Nature 465, 507–510. https://doi.org/10.1038/nature08870.

Juaire, K.D., Lapouge, K., Becker, M.M.M., Kotova, I., Michelhans, M., Carapito, R., Wild, K., Bahram, S., Sinning, I., 2021. Structural and functional impact of SRP54 mutations causing severe congenital neutropenia. Structure 29, 15–28.e7. https://doi.org/10.1016/j.str.2020.09.008.

Kato, H., Takeuchi, O., Mikamo-Satoh, E., Hirai, R., Kawai, T., Matsushita, K., Hiiragi, A., Dermody, T.S., Fujita, T., Akira, S., 2008. Length-dependent recognition of double-stranded ribonucleic acids by retinoic acid–inducible gene-I and melanoma differentiation–associated gene 5. J. Exp. Med. 205, 1601–1610. https://doi.org/10.1084/jem.20080091.

Kawai, T., Ikegawa, M., Ori, D., Akira, S., 2024. Decoding Toll-like receptors: recent insights and perspectives in innate immunity. Immunity 57, 649–673. https://doi.org/10.1016/j.immuni.2024.03.004.

Kowalinski, E., Lunardi, T., McCarthy, A.A., Louber, J., Brunel, J., Grigorov, B., Gerlier, D., Cusack, S., 2011. Structural basis for the activation of innate immune pattern-recognition receptor RIG-I by viral RNA. Cell 147, 423–435. https://doi.org/10.1016/j.cell.2011.09.039.

Li, D., 2021. Pattern recognition receptors in health and diseases. Signal Transduct. Targeted Ther. https://doi.org/10.1038/s41392-021-00687-0.

Li, J., Zhang, X., Xu, J., Pei, X., Wu, Z., Wang, T., Yin, S., 2019. iTRAQ analysis of liver immune-related proteins from darkbarbel catfish (Pelteobagrus vachelli) infected with Edwardsiella ictaluri. Fish Shellfish Immunol. 87, 695–704. https://doi.org/10.1016/j.fsi.2019.01.036.

Li, S., Yang, J., Zhu, Y., Wang, H., Ji, X., Luo, J., Shao, Q., Xu, Y., Liu, X., Zheng, W., Meurens, F., Chen, N., Zhu, J., 2021. Analysis of porcine RIG-I like receptors revealed the positive regulation of RIG-I and MDA5 by LGP2. Front. Immunol. 12, 609543 https://doi.org/10.3389/fimmu.2021.609543.

Li, T., Cai, Y., Li, C., Huang, J., Chen, J., Zhang, Z., Cao, R., Zhou, B., Feng, X., 2023. MDA5 with Complete CARD2 Region Inhibits the Early Replication of H9N2 AIV and Enhances the Immune Response during Vaccination.

Lian, H., Zang, R., Wei, J., Ye, W., Hu, M.-M., Chen, Y.-D., Zhang, X.-N., Guo, Y., Lei, C.-Q., Yang, Q., Luo, W.-W., Li, S., Shu, H.-B., 2018. The zinc-finger protein ZCCHC3 binds RNA and facilitates viral RNA sensing and activation of the RIG-I-like receptors. Immunity 49, 438–448.e5. https://doi.org/10.1016/j.immuni.2018.08.014.

Liu, Y., Xiao, J., Qiao, G., Wang, Q., Yang, X., Xu, X., Li, J., Zhang, J., Chang, M., Feng, H., 2022. DDX19 inhibits RLR/IRF3 mediated type I interferon signaling of black carp Mylopharyngodon piceus by restricting IRF3 from entering nucleus. Aquaculture 553, 738087. https://doi.org/10.1016/j.aquaculture.2022.738087.

Luirink, J., 2004. SRP-mediated protein targeting: structure and function revisited. Biochim. Biophys. Acta Mol. Cell Res. https://doi.org/10.1016/j.bbamcr.2004.03.013.

Rehwinkel, J., 2020. RIG-I-like receptors: their regulation and roles in RNA sensing. Nat. Rev. Immunol. 20 (9), 537–551. https://doi.org/10.1038/s41577-020-0288-3.

Sanchez David, R.Y., Combredet, C., Najburg, V., Millot, G.A., Beauclair, G., Schwikowski, B., Léger, T., Camadro, J.-M., Jacob, Y., Bellalou, J., Jouvenet, N., Tangy, F., Komarova, A.V., 2019. LGP2 binds to PACT to regulate RIG-I– and MDA5-mediated antiviral responses. Sci. Signal. 12, eaar3993 https://doi.org/10.1126/scisignal.aar3993.

Schroeder, H.W., Cavacini, L., 2010. Structure and function of immunoglobulins. J. Allergy Clin. Immunol. 125, S41–S52. https://doi.org/10.1016/j.jaci.2009.09.046.

Schürch, C., Schaefer, T., Müller, J.S., Hanns, P., Arnone, M., Dumlin, A., Schärer, J., Sinning, I., Wild, K., Skokowa, J., Welte, K., Carapito, R., Bahram, S., Konantz, M., Lengerke, C., 2021. *SRP54* mutations induce congenital neutropenia via dominant-negative effects on *XBP1* splicing. Blood 137, 1340–1352. https://doi.org/10.1182/blood.2020008115.

Sharma, A., Kontodimas, K., Bosmann, M., 2021. The MAVS immune recognition pathway in viral infection and sepsis. Antioxidants Redox Signal. 35, 1376–1392. https://doi.org/10.1089/ars.2021.0167.

Song, B., Chen, Y., Liu, X., Yuan, F., Tan, E.Y.J., Lei, Y., Song, N., Han, Y., Pascal, B.D., Griffin, P.R., Luo, C., Wu, B., Luo, D., Zheng, J., 2021. Ordered assembly of the cytosolic RNA-sensing MDA5-MAVS signaling complex via binding to unanchored K63-linked poly-ubiquitin chains. Immunity 54, 2218–2230.e5. https://doi.org/10.1016/j.immuni.2021.09.008.

Wang, C., Li, J., Yang, X., Wang, Q., Zhong, H., Liu, Y., Yan, W., He, Y., Deng, Z., Xiao, J., Feng, H., 2021. Black carp IKKε collaborates with IRF3 in the antiviral signaling. Fish Shellfish Immunol. 118, 160–168. https://doi.org/10.1016/j.fsi.2021.08.034.

Wang, D.-P., 2021. SRP54 negatively regulates IFN-beta production and antiviral response by targeting RIG-I and MDA5. Virol. Sin. 36 (2), 231–240. https://doi.org/10.1007/s12250-020-00267-6.

Watanabe, Y., Uruha, A., Suzuki, S., Nakahara, J., Hamanaka, K., Takayama, K., Suzuki, N., Nishino, I., 2016. Clinical features and prognosis in anti-SRP and anti-HMGCR necrotising myopathy. ournal of neurology, neurosurgery, and psychiatry 87 (10). https://doi.org/10.1136/jnnp-2016-313418.

Wei, Z., 2020. Regulation of MAVS expression and signaling function in the antiviral innate immune response. Front. Immunol. 11 https://doi.org/10.3389/fimmu.2020.01030.

Wu, H., Liu, L., Wu, S., Wang, C., Feng, C., Xiao, J., Feng, H., 2018. IFNb of black carp functions importantly in host innate immune response as an antiviral cytokine. Fish Shellfish Immunol. 74, 1–9. https://doi.org/10.1016/j.fsi.2017.12.049.

Zhang, J., Sun, Z., Su, W., Wang, Z., Meng, W., Chang, Y., 2023. A signal recognition particle receptor gene from the sea cucumber, Apostichopus japonicas. Sci. Rep. 13, 22973 https://doi.org/10.1038/s41598-023-50320-z.

Zhang, Y., Jiang, J., Chen, Y., Zhu, R., Shi, Y., Zhang, Q., Gui, J., 2007. The innate immune response to grass carp hemorrhagic virus (GCHV) in cultured Carassius auratus blastulae (CAB) cells. Dev. Comp. Immunol. 31, 232–243. https://doi.org/10.1016/j.dci.2006.05.015.